

# Elastic gauge fields and zero-field 3D quantum Hall effect in hyperhoneycomb lattices

Sang Wook Kim and Bruno Uchoa

*Department of Physics and astronomy, University of Oklahoma, Norman, Oklahoma 73019, USA*

(Dated: January 4, 2019)

We derive the elastic gauge fields that emerge from lattice deformations in the hyperhoneycomb lattice, a three dimensional (3D) structure with trigonally connected sites. In its semimetallic form, this lattice is a nodal-line semimetal with a closed loop of Dirac nodes. Using strain engineering, we find a whole family of strain deformations that create uniform nearly flat Landau levels. In the 3D quantum anomalous Hall phase, we show that the elastic Hall viscosity on the plane of the nodal line is  $\eta_H = \beta^2 \sqrt{3} / (8\pi a^3)$ , where  $a$  is the lattice constant.

*Introduction.* In honeycomb lattices such as graphene [1], strain deformations couple to electronic degrees of freedom as gauge fields and can induce Landau level (LL) quantization with very large effective pseudomagnetic fields [2–5]. When the chemical potential is inside the gap of the LLs, the Hall conductivity per valley is quantized and the system is expected to show a zero-field quantum Hall effect (QHE). Due to the dispersion of the LLs, Hall conductivity quantization is not common in three dimensions (3D), and may occur only in extremely anisotropic systems such as Bechgaard salts [6, 7], Bernal graphite [8, 9], and in nodal-line semimetals [10–12].

In this Rapid communication, we derive the elastic gauge fields that follow from arbitrary lattice deformations in the hyperhoneycomb lattice, a natural 3D generalization of the honeycomb geometry where all sites are connected by coplanar trigonal bonds, as shown in Fig. 1a. In the semimetallic form, this lattice is an example of a nodal-line semimetal [10, 13–18]. We identify a whole family of lattice deformations that produce uniform nearly flat LLs in 3D, a prerequisite for the 3D zero-field QHE. In the 3D quantum anomalous Hall (QAH) phase [19], which is the extension of the Haldane model [20] to the hyperhoneycomb lattice, we also calculate the elastic Hall viscosity  $\eta_H$ . Also known as the phonon Hall viscosity [21], this quantity is analogous to the dissipationless viscous response of electrons in the quantum Hall regime [22–24] and is topological in nature. We show that  $\eta_H = \beta^2 \sqrt{3} / (8\pi a^3)$  on the plane of the nodal line, where  $\beta$  is an elastic parameter and  $a$  is the lattice constant.

*Hamiltonian.* The hyperhoneycomb lattice has four sites per unit cell  $\mu = 1, \dots, 4$  and is generated by the lattice vectors  $\mathbf{a}_1 = (\sqrt{3}, 0, 0)$ ,  $\mathbf{a}_2 = (0, \sqrt{3}, 0)$ , and  $\mathbf{a}_3 = (-\sqrt{3}/2, \sqrt{3}/2, 3)$ , in units of the lattice constant  $a$ . In the momentum space, the reciprocal lattice is generated by the vectors  $\mathbf{b}_1 = (2\pi/\sqrt{3}, 0, -\pi/3)$ ,  $\mathbf{b}_2 = (0, -2\pi/\sqrt{3}, \pi/3)$  and  $\mathbf{b}_3 = (0, 0, 2\pi/3)$ , shown in Fig. 1b. The tight-binding Hamiltonian is a  $4 \times 4$  matrix [10]

$$\mathcal{H}_{0,\mu\nu}(\mathbf{k}) = -t_0 \sum_{\vec{\delta}_{\mu\nu}} e^{i\mathbf{k}\cdot\vec{\delta}_{\mu\nu}}, \quad (1)$$

where  $t_0$  is the hopping amplitude,  $\vec{\delta}_{\mu\nu}$  are the nearest neighbor (NN) vectors between sites of species  $\mu$  and  $\nu$

and  $\mathbf{k}$  is the momentum measured from the center of the Brillouin zone (BZ). In total, there are six NN vectors  $\vec{\delta}_{12} = (\pm\sqrt{3}a/2, 0, a/2)$ ,  $\vec{\delta}_{34} = (0, \pm\sqrt{3}a/2, a/2)$ ,  $\vec{\delta}_{14} = (0, 0, -a)$  and  $\vec{\delta}_{23} = (0, 0, a)$ . The low energy bands of this lattice have a line of Dirac nodes  $\mathbf{k}_0 = [k_x(s), k_y(s), 0]$  in the  $k_z = 0$  plane, which can be written in terms of some parameter  $s$  that satisfies the equation  $4 \cos[3k_x(s)/2] \cos[3k_y(s)/2] = 1$ . The low energy projected Hamiltonian is described by a  $2 \times 2$  matrix expanded around the nodal line

$$\mathcal{H}_{0,p}(\mathbf{q}) = [v_x(s)q_x + v_y(s)q_y] \sigma_1 + v_z(s)q_z \sigma_2 \quad (2)$$

where  $\mathbf{q} \equiv \mathbf{k} - \mathbf{k}_0(s)$  is the relative momentum,  $\sigma_1$ ,  $\sigma_2$  are the two off-diagonal Pauli matrices and

$$\begin{aligned} v_x(s) &= \frac{\sqrt{3}}{1 + \alpha^2} \sin\left(\frac{\sqrt{3}}{2}k_x(s)\right) t_0 \\ v_y(s) &= \frac{\alpha^2 \sqrt{3}}{1 + \alpha^2} \sin\left(\frac{\sqrt{3}}{2}k_y(s)\right) t_0 \\ v_z(s) &= -\frac{3\alpha}{1 + \alpha^2} t_0, \end{aligned} \quad (3)$$

are the velocities of the quasiparticles, with  $\alpha(s) \equiv 2 \cos[\sqrt{3}k_x(s)a/2]$  [19]. The energy spectrum of the

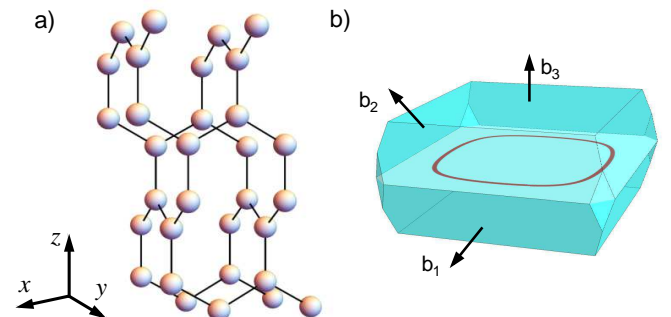


Figure 1. a) Hyperhoneycomb lattice, with four atoms per unit cell. All sites are linked by coplanar trigonal bonds spaced by  $120^\circ$ . b) Brillouin zone (BZ) of the hyperhoneycomb lattice, with the nodal line shown in red. The arrows show the reciprocal lattice vectors.

quasiparticles is  $E_0(\mathbf{q}) = \pm \sqrt{(v_x q_x + v_y q_y)^2 + v_z^2 q_z^2}$ . The wavefunctions have a  $\pi$  Berry phase for closed line trajectories that encircle the nodal loop.

*Elastic gauge fields.* The inclusion of lattice deformations can be done by locally changing the distance between lattice sites, which affect value of the hopping constant. Expanding it to lowest order in the displacement of the lattice,

$$t \left( \vec{\delta}^{(n)} + \delta \mathbf{r} \right) \approx t_0 + \frac{\beta}{a^2} \delta_i^{(n)} \delta_j^{(n)} u_{ij} + \mathcal{O}(\delta r^2), \quad (4)$$

with  $n = 1, \dots, 6$  indexing the 6 NN lattice vectors  $\vec{\delta}^{(n)}$ ,  $u_{ij} = \frac{1}{2}(\partial_i u_j + \partial_j u_i)$  is the strain tensor defined in terms of the displacement field  $\mathbf{u}$  of the lattice and  $\beta = a \frac{\partial t}{\partial r} = \frac{\partial \log t}{\partial \log r}$  is the Grüneisen parameter of the model. Including the lattice distortions in Hamiltonian (5), one gets two terms,  $\mathcal{H}_p = \mathcal{H}_{0,p} + \mathcal{H}_{el}$ , where

$$\mathcal{H}_{el} = \frac{3\beta}{4a} v_z (u_{xx} + u_{yy} - 2u_{zz}) \sigma_1 - \frac{\beta}{a} (v_x u_{xz} + v_y u_{yz}) \sigma_2 \quad (5)$$

is the elastic contribution. As in the 2D case (graphene), the deformation of the lattice couples to the Dirac fermions as an elastic gauge field  $\mathbf{A}$ . It is convenient to rewrite the Hamiltonian in the more familiar form

$$\mathcal{H}_p(\mathbf{q}) = [v_x (q_x + A_x) + v_y (q_y + A_y)] \sigma_1 + v_z (q_z + A_z) \sigma_2, \quad (6)$$

where

$$\begin{aligned} A_x(s) &= \frac{v_x v_z}{v_\rho^2} \frac{3\beta}{4a} (u_{xx} + u_{yy} - 2u_{zz}) \\ A_y(s) &= \frac{v_y v_z}{v_\rho^2} \frac{3\beta}{4a} (u_{xx} + u_{yy} - 2u_{zz}) \\ A_z(s) &= -\frac{\beta}{a} \left( \frac{v_x}{v_z} u_{xz} + \frac{v_y}{v_z} u_{yz} \right) \end{aligned} \quad (7)$$

are the components of the elastic gauge field along the nodal line, with  $v_\rho^2(s) = v_x^2(s) + v_y^2(s)$ . The definition of the  $A_x$  and  $A_y$  components is to a degree arbitrary. In (7) we chose the most symmetric combination, although this choice has no effect in physical observables.

Those gauge fields can be associated to a pseudomagnetic field  $\mathbf{B} = \nabla \times \mathbf{A}$ , which follows from lattice deformations and hence must preserve time reversal symmetry (TRS). While pseudo magnetic fields couple to the Dirac fermions similarly to conventional magnetic fields and can produce Landau level (LL) quantization, they create a zero net magnetic flux at each lattice site. Therefore, electrons sitting at opposite points in the nodal line are related by TRS and must necessarily couple to opposite  $\mathbf{B}$  fields.

*Strain engineering.* In order to produce zero-field quantum Hall effect, one needs to create 3D LL quantization with well defined gaps in between. In 2D, the conventional Hall conductivity  $\sigma_{xy}$  is a dimensionless and quantized in units of  $e^2/h$ . In 3D, it has an extra unit of inverse length. According to Halperin [25], the Hall conductivity tensor is  $\sigma_{ij} = e^2/(2\pi\hbar)\epsilon_{ijk}G_k$ , where  $\mathbf{G}$  is a

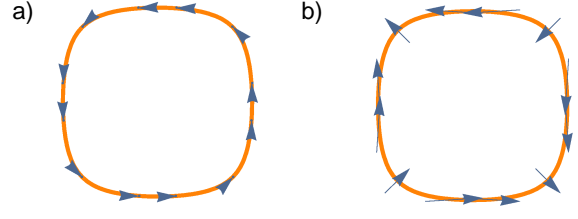


Figure 2. Pseudomagnetic field  $\mathbf{B}$  along the nodal line for two different strain field configurations. a)  $\mathbf{u} = (2xz, 2yz, 0)$  and b)  $\mathbf{u} = (2yz, 2xz, 0)$ . Both configurations lead to uniform  $\mathbf{B}$  fields in real space, but only the former produces nearly flat LLs.

reciprocal lattice vector (and could be zero). In general, a finite Hall conductivity in 2D (3D) is allowed whenever the chemical potential is in the gap between different LLs, and implies in the existence of chiral edge (surface) states. At zero field, the Hall conductivity tensor due to pseudomagnetic fields does not create chiral charge currents as in the conventional quantum Hall effect, but rather a valley current.

*Spectrum of Landau levels.* In all possible strain configurations, the effective Hamiltonian (6) has the form  $\mathcal{H}_p(\mathbf{q}) = h_1 \sigma_1 + h_2 \sigma_2$ . In specific, for configuration  $\mathbf{u} = (2xz, 2yz, 0)$ ,

$$h_1 = v_x q_x + v_y q_y + \frac{3\beta}{a} v_z z \quad (8)$$

$$h_2 = v_z q_z - \frac{\beta}{a} v_x x - \frac{\beta}{a} v_y y. \quad (9)$$

The corresponding pseudomagnetic field  $\mathbf{B} = (-v_y/v_z - 3v_y v_z/v_\rho^2, v_x/v_z + 3v_x v_z/v_\rho^2, 0)$  forms a closed lines in the BZ around the nodal line, as shown in Fig. 2a. In order to calculate the spectrum of Landau levels, we define the canonically conjugated ladder operators  $a = \frac{1}{\omega} (h_1 + i h_2)$  and  $a^\dagger = \frac{1}{\omega} (h_1 - i h_2)$ , which satisfy  $[a, a^\dagger] = i[h_2, h_1]/\omega^2 = 1$ . The parameter

$$\omega(s) = \sqrt{2 \frac{\beta}{a} [v_x^2(s) + v_y^2(s) + 3v_z^2(s)]^{\frac{1}{2}}}, \quad (10)$$

is the analog of the cyclotronic frequency. Taking the square of the Hamiltonian,  $\mathcal{H}_0^2 = \omega^2 [a^\dagger a + \frac{1}{2}] 1_{2 \times 2} - \frac{1}{2} \omega^2 \sigma_3$ , that results in the spectrum of LLs parametrized along the nodal line,

$$E_N(s) = \text{sgn}(N) \omega(s) \sqrt{|N|}, \quad (11)$$

as shown in Fig. 3a. The energy spectrum has a zeroth LL, as expected for Dirac fermions, and a clear gap between the first few LLs. That permits the emergence of a zero-field QHE due to strain whenever the chemical potential lays in the LL gap. For the strain configuration shown in Fig. 2b,  $\mathbf{u} = (2yz, 2xz, 0)$ , the parameter  $\omega(s) = \sqrt{(\beta/a)v_x(s)v_y(s)}$  has zeros along the nodal line, where all LLs collapse. In that configuration, although

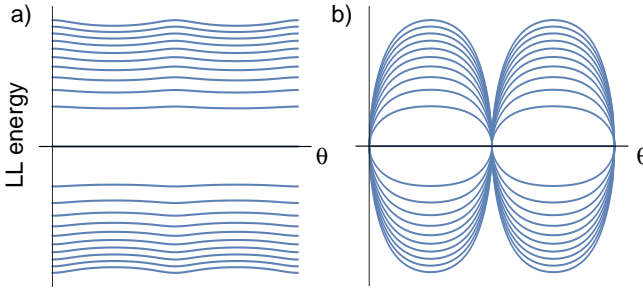


Figure 3. Energy of the Landau levels around the nodal line vs. polar angle  $\theta$ ,  $(0 \leq \theta < \pi)$  for two strain configurations: (a)  $\mathbf{u} = (2xz, 2yz, 0)$  and (b)  $\mathbf{u} = (2yz, 2xz, 0)$ . The former configuration belongs to a broader family of deformations that produce nearly flat LLs in 3D.

the LLs are well defined away from those points, their dispersion does not lead to a well defined gap in the excitation spectrum, and hence the system does not have a zero-field QAH effect.

In general, introducing the positive constants  $c_1$  and  $c_2$ , one can build a whole family of strain deformations

$$\mathbf{u} = (c_1 xz, c_2 yz, 0), \quad (12)$$

that lead to uniform nearly flat LLs in 3D [26]. In this family,  $\omega(s) = \sqrt{i[h_2, h_1]}$  is non zero for all points along the nodal line. The energy spectrum has the same form as in Eq. (11), with  $\omega(s) = \sqrt{(\beta/a)[c_1 v_x^2(s) + c_2 v_y^2(s) + \frac{3}{2}(c_1 + c_2)v_z^2(s)]}$ . In the special case  $c_1 = c_2 = 2$ , the configuration of strain forces acting on a sample with cylindrical geometry are illustrated in Fig. 4. The arrows in panel 4a indicate the orientation of the strain forces acting on the crystal.

*Elastic Hall viscosity.* In quantum Hall systems, the Hall viscosity follows from the linear response of the system to gravitational fluctuations, which manifest through local changes in the metric of space  $\xi_{ij} = \frac{1}{2}(\partial_i \xi_j + \partial_j \xi_i)$ , where  $\xi_i$  has the physical meaning of a strain field. The so called gravitational Hall viscosity is defined as the variation of the stress tensor  $T_{\mu\nu} = \partial \mathcal{H} / \partial \xi_{\mu\nu}$  to time variations of the strain tensor  $\dot{\xi}_{ij}$ . By analogy, the elastic (phonon) Hall viscosity can be derived using linear response as [21–23]

$$\left\langle \frac{\partial \mathcal{H}_p}{\partial u_{\mu\nu}} \right\rangle = \lambda_{\mu\nu\rho\gamma} u_{\rho\gamma} + \eta_{\mu\nu\rho\gamma} \dot{u}_{\rho\gamma} \quad (13)$$

where  $\langle \dots \rangle$  integrates over the fermions,  $\lambda_{\mu\nu\rho\gamma}$  is the elastic moduli,  $\dot{u}_{\rho\gamma}$  the strain-rate tensor and  $\eta_{\mu\nu\rho\gamma}$  the elastic Hall viscosity tensor. The first term is the elastic response of a charge neutral fluid and the second one the viscous response [22, 23]. As the stress tensor, the tensors  $u$ ,  $\dot{u}$  are symmetric, while the viscosity tensor is symmetric under  $\mu \leftrightarrow \nu$  or  $\rho \leftrightarrow \gamma$ . However, with respect to the exchange  $\mu\nu \leftrightarrow \rho\gamma$ , the viscosity tensor has a symmetric part  $\eta_{\mu\nu\rho\gamma}^S = \eta_{\rho\gamma\mu\nu}^S$  and an antisymmetric

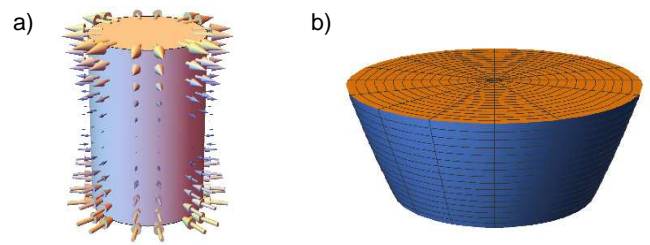


Figure 4. Elastic deformation of a cylinder under the strain configuration  $\mathbf{u} = (2xz, 2yz, 0)$ . The arrows in panel a indicate the strain forces that create uniform nearly flat LLs in a 3D material (b).

one  $\eta_{\mu\nu\rho\gamma}^A = -\eta_{\rho\gamma\mu\nu}^A$ . The symmetric part is associated with dissipation and vanishes at zero temperature. The antisymmetric one describes a non-dissipative response with topological nature and is non-zero only when TRS is broken. In general, one can calculate the antisymmetric viscosity tensor from the effective action

$$\delta S_H = \frac{1}{2} \int d^3x dt \eta_{\mu\nu\rho\gamma} u_{\mu\nu} \dot{u}_{\rho\gamma}, \quad (14)$$

which resembles a Chern-Simons action for the usual QHE [27, 28].

We will consider the elastic Hall viscosity for the 3D QAH state, which is an extension of the Haldane model for the hyperhoneycomb lattice, described in detail in ref. [19]. For nodal line semimetals, loop currents on the lattice can create a mass term around the nodal line with the general form

$$\mathcal{H}_m(\mathbf{q}) = \left[ m(s) + \sum_{i=x,y,z} v'_i(s) q_i \right] \sigma_3, \quad (15)$$

where  $v'_i(s)$  gives the mass dispersion in the  $i = x, y, z$  direction. The Haldane mass  $m(s)$  changes sign at  $2(2n+1)$  points along the nodal line, with  $n \in \mathbb{N}$ , breaking inversion and TRS symmetry [19, 29]. The nodes of the mass, where  $m(s) = 0$ , are Weyl points with a well defined helicity [19]. Weyl points with opposite helicities are connected by surface states in the form of topological Fermi arcs [30].

*Effective action.* In the QAH state, the Hamiltonian away from the Weyl points of the nodal line has the form

$$\mathcal{H}_{QAH}(\mathbf{q}) = \mathcal{H}_p(\mathbf{q}) + m(s) \sigma_3. \quad (16)$$

The effective action in terms of the strain tensor  $u_{ij}$  can be derived by integrating out the fermions. That results in the effective action  $S_{\text{ef}}(u) = \text{Tr} [\ln (G^{-1})]$ , where  $G^{-1}(q) = iq_0 - \mathcal{H}_{QAH}(\mathbf{q}) \equiv G_0^{-1}(q) - \Sigma_{\text{el}}$  is the Green's function and

$$\Sigma_{\text{el}}(u) = v_z A_1 \sigma_1 + (v_x A_2 + v_y A'_2) \sigma_2 \quad (17)$$

is the self-energy due to elastic terms. For convenience, we defined the elastic gauge fields in (5) as  $A_1 = -\frac{\beta}{a} \frac{3}{4} (u_{xx} + u_{yy} - 2u_{zz})$ ,  $A_2 = -\frac{\beta}{a} u_{xz}$  and  $A'_2 = -\frac{\beta}{a} u_{yz}$ .

Expanding the action in powers of the elastic gauge fields, namely  $S_{\text{ef}} = \text{tr} \ln G_0^{-1} - \text{tr} \sum_{n=0}^{\infty} \frac{1}{n} (G_0 \Sigma)^n$ , the lowest order contribution to the Hall viscosity comes from two loop,  $S_{\text{ef}}^{(2)} = -\frac{1}{2} \text{tr} [G_0 \Sigma G_0 \Sigma]$ . More explicitly,

$$\delta S_{\text{ef}} = -\frac{1}{2} \int \frac{d^4 k}{(2\pi)^4} [v_x v_z A_1(-k) \Pi^{12}(k) A_2(k) + v_y v_z A_1(-k) \Pi^{12}(k) A'_2(k) + (1 \leftrightarrow 2)], \quad (18)$$

where  $\Pi^{\mu\nu}(k) = \int \frac{d^4 q}{(2\pi)^4} \text{tr} [G_0(q+k) \sigma_\mu G_0(q) \sigma_\nu]$  is the standard polarization tensor, with antisymmetric off-diagonal terms,  $\Pi^{12}(k) = -\Pi^{21}(k)$ . Integration can be done by slicing the BZ into planes intersecting the nodal line at two points. Integrating over a slice in the  $xz$  plane for the first term,

$$v_x v_z \Pi^{12}(k) = \frac{k_0}{2\pi} \int_C \frac{dq_y}{(2\pi)} \nu_{(y)}(\mathbf{q}_0) = -\frac{k_0}{2\pi} \lambda_y, \quad (19)$$

where  $\nu_{(y)}(\mathbf{k}_0) = \frac{1}{2} \text{sign}[v_x(s)v_z(s)m(s)] = \pm \frac{1}{2}$  is the topological charge of 2D massive Dirac fermions confined to an  $xz$  plane crossing the nodal line at  $\mathbf{k}_0$ . Integration along the nodal loop  $C$  gives the  $y$  component of the Chern vector  $\lambda = (\lambda_x, \lambda_y, \lambda_z)$ , which belongs to the reciprocal lattice  $\mathbf{G}$  and sets the 3D quantum Hall conductivity of the system,  $\sigma_{ij} = e^2/(2\pi\hbar) \epsilon_{ijk} \lambda_k$ . From a similar argument,  $v_y v_z \Pi^{12}(k) = -v_y v_z \Pi^{21}(k) = \lambda_x$ . Hence,

$$\delta S_{\text{ef}} = \frac{1}{16\pi^2} \int \frac{d^4 k}{(2\pi)^4} [-\lambda_x A_1(-k) k_0 A'_2(k) + \lambda_y A_1(-k) k_0 A_2(k) - (1 \leftrightarrow 2)]. \quad (20)$$

Performing the substitution  $A_1 = d_z$ ,  $A_2 = d_x$  and  $A'_2 = d_y$ , the effective action can be written in a more compact form,

$$\delta S_{\text{ef}} = \frac{1}{16\pi^2} \int d^4 x \epsilon^{\mu\nu\rho} \lambda_\mu d_\nu \dot{d}_\rho, \quad (21)$$

where

$$\begin{aligned} d_x &= -\frac{\beta}{a} u_{xz} \\ d_y &= -\frac{\beta}{a} u_{yz} \\ d_z &= -\frac{\beta}{a} \frac{3}{4} (u_{xx} + u_{yy} - 2u_{zz}). \end{aligned} \quad (22)$$

For the hyperhoneycomb lattice, the Chern vector is  $\lambda = \mathbf{b}_1 + \mathbf{b}_2 = (2\pi/\sqrt{3}, -2\pi/\sqrt{3}, 0) a^{-1}$  [19]. Writing the action in a more explicit form,

$$\delta S_{\text{ef}} = \frac{1}{2} \int d^4 x \eta_H [(u_{xx} + u_{yy} - 2u_{zz})(\dot{u}_{yz} + \dot{u}_{xz}) - (u_{yz} + u_{xz})(\dot{u}_{xx} + \dot{u}_{yy} - 2\dot{u}_{zz})], \quad (23)$$

with  $\eta_H = \beta^2 \sqrt{3}/8\pi a^3$ . The action can be cast in the form of (14), where the elastic Hall viscosity tensor is  $\eta_{xxxx} = \eta_{xxyz} = \eta_{yyxz} = \eta_{yyyz} = \eta_H$ , and  $\eta_{zzxz} = \eta_{zzyz} = -2\eta_H$ . The elastic Hall viscosity tensor is hence anisotropic, as expected in 3D [23]. The existence of a dissipationless viscosity at zero temperature reflects the topological nature of the QAH state.

*Experimental observation.* Although there are no known examples of semimetallic hyperhoneycomb crystals [31], this lattice may be artificially created in optical lattices [32], and also in photonic [4, 33] and acoustic metamaterials [34]. In synthetic lattices, strain deformations can be readily implemented with local displacements of the lattice sites, without the need to apply pressure. While local probes such as scanning tunneling spectroscopy can fully characterize the LLs in 2D [2, 3], this method can be used to characterize the surface states of the LLs in the 3D case.

In quantum Hall systems, the measurement of the Hall viscosity is typically challenging [35], as it involves probing the response of the stress tensor under changes of the space metric [23]. In Galilean invariant systems in the hydrodynamic regime, the Hall viscosity can be determined solely in terms of the electromagnetic response due to a non-homogeneous electric field [36, 37]. The elastic Hall viscosity nevertheless can be measured in terms of the dispersion of sound waves. When  $\eta_H = \eta_{xxxx}$  is zero, the longitudinal and transverse modes are decoupled at long wavelengths. In the topological phase, where  $\eta_H$  is finite, the transverse and longitudinal modes are expected to mix, allowing one to measure the elastic Hall viscosity through the corrections to the dispersion of the phonons [21]. The quantum simulation of Chern insulating phases has been done in honeycomb lattices of cold atoms [32], in quantum circuits [38] and acoustic metamaterials [34]. We conjecture that the QAH state in 3D may be experimentally realized in synthetic lattices as well.

*Conclusions.* We have derived the elastic gauge fields that are created due to lattice deformations in the hyperhoneycomb lattice. We proposed a family of strain configurations that lead to uniform nearly flat LLs in 3D. We have also shown that the elastic Hall viscosity for this lattice in the 3D QAH state is  $\eta_H = \beta^2 \sqrt{3}/(8\pi a^3)$  on the plane of the nodal line.

*Acknowledgements.* SWK thanks X. Dou for helpful discussions. BU and SWK acknowledge NSF CAREER grant No DMR-1352604 for support.

[1] A. H. Castro Neto, N. M. R. Peres, F. Guinea, A. Geim, K. Novoselov, Rev. Mod. Phys. **81**, 109 (2009).

[2] N. Levy, S. A. Burke, K. L. Meaker, M. Panlasigui, A.

Zettl, F. Guinea, A. H. Castro Neto, M. F. Crommie, *Science* **329**, 544 (2010).

[3] K. K. Gomes, W. Mar, Wonhee Ko, F. Guinea, H. C. Manoharan, *Nature* **483**, 306 (2012).

[4] M. C. Rechtsman, J. M. Zeuner, A. Tunnermann, S. Nolte, M. Segev and A. Szameit, *Nat. Photonics* **7**, 153 (2013).

[5] F. Guinea, M. I. Katsnelson and A. K. Geim, *Nat. Phys.* **6**, 30 (2010).

[6] L. Balicas, G. Kriza, and F. I. B. Williams, *Phys. Rev. Lett.* **75**, 2000 (1995).

[7] S. M. McKernan, S. T. Hannahs, U. M. Scheven, G. M. Danner, and P. M. Chaikin, *Phys. Rev. Lett.* **75**, 1630 (1995).

[8] B. A. Bernevig, T. L. Hughes, S. Raghu, and D. P. Arovas, *Phys. Rev. Lett.* **99**, 146804 (2007).

[9] D. Arovas and F. Guinea, *Phys. Rev. B* **78**, 245416 (2008).

[10] K. Mullen, B. Uchoa, and D. T. Glatzhofer, *Phys. Rev. Lett.* **115**, 026403 (2015).

[11] L.-K. Lim and R. Moessner, *Phys. Rev. Lett.* **118**, 016401 (2017).

[12] J.-W. Rhim and Y. B. Kim, *Phys. Rev. B* **92**, 045126 (2015).

[13] Y. Kim, B. J. Wieder, C. L. Kane, and A. M. Rappe, *Phys. Rev. Lett.* **115**, 036806 (2015).

[14] H. Weng, Y. Liang, Q. Xu, R. Yu, Z. Fang, X. Dai, and Y. Kawazoe, *Phys. Rev. B* **92**, 045108 (2015).

[15] R. Yu, H. Weng, Z. Fang, X. Dai, and X. Hu, *Phys. Rev. Lett.* **115**, 036807 (2015).

[16] T. T. Heikkila and G. E. Volovik, *JETP Lett.* **93**, 59 (2011).

[17] Y. Chen, Y. Xie, S. A. Yang, H. Pan, F. Zhang, M. L. Cohen, and S. Zhang, *Nano Lett.* **15**, 6974 (2015).

[18] L. S. Xie, L. M. Schoop, E. M. Seibel, Q. D. Gibson, W. Xie, and R. J. Cava, *APL Mater.* **3**, 083602 (2015).

[19] S. W. Kim, K. Seo, B. Uchoa, *Phys. Rev. B* **97**, 201101(R) (2018).

[20] D. Haldane, *Phys. Rev. Lett.* **61**, 2015 (1988).

[21] M. Barkeshli, S. Bum Chung, and X.-L. Qi, *Phys. Rev. B* **85**, 245107 (2012).

[22] J. E. Avron, R. Seiler, and P. G. Zograf, *Phys. Rev. Lett.* **75**, 697 (1995).

[23] J. E. Avron, *J. Stat. Phys.* **92**, 543 (1998).

[24] N. Read and E. Rezayi, *Phys. Rev. B* **84**, 085316 (2011).

[25] B. I. Halperin, *Jpn. J. Appl. Phys.* **26**, 1913 (1987).

[26] From (7), strain fields that create uniform  $\mathbf{B}$  fields must satisfy  $u_{xz} = c_1 x$ ,  $u_{yz} = c_2 y$  and  $u_{xx} + u_{yy} - 2u_{zz} = c_3 z$ , with  $c_3$  another constant. Nearly flat LLs with finite gaps in between require that  $[h_1, h_2] \neq 0$  at all points of the nodal line. By inspection, the later condition can be satisfied for any positive constants  $c_1$ ,  $c_2$  and  $c_3$ .

[27] T. L. Hughes, R. G. Leigh, and E. Fradkin, *Phys. Rev. Lett.* **107**, 075502 (2011).

[28] A. Cortijo, Y. Ferreira, K. Landsteiner, and M. A. H. Vozmediano, *Phys. Rev. Lett.* **115**, 177202 (2015).

[29] R. Okugawa and S. Murakami, *Phys. Rev. B* **96**, 115201 (2017).

[30] N. P. Armitage, E. J. Mele, and Ashvin Vishwanath, *Rev. Mod. Phys.* **90**, 015001 (2018).

[31] K. A. Modic et al., *Nat. Commun.* **5**, 4203 (2014).

[32] G. Jotzu, M. Messer, R. Desbuquois, M. Lebrat, T. Uehlinger, D. Greif, and T. Esslinger, *Nature (London)* **515**, 237 (2014).

[33] L. Lu, L. Fu, J. D. Joannopoulos, and M. Soljačić, *Nat. Photonics* **7**, 294 (2013).

[34] Y. Zhu, Y. Peng, X. Fan, J. Yang, B. Liang, X. Zhu, J. Cheng, arXiv:1801.07942 (2018).

[35] A. I. Berdyugin, S. G. Xu, F. M. D. Pellegrino, R. Krishna Kumar, A. Principi, I. Torre, M. Ben Shalom, T. Taniguchi, K. Watanabe, I. V. Grigorieva, M. Polini, A. K. Geim, D. A. Balandin, arXiv:1806.01606 (2018).

[36] C. Hoyos, and D. T. Son, *Phys. Rev. Lett.* **108**, 066805 (2012).

[37] F. D. M. Haldane, arXiv:0906.1854 (2009).

[38] P. Roushan et al., *Nature (London)* **515**, 241 (2014).